ISSN 1070-3632, Russian Journal of General Chemistry, 2015, Vol. 85, No. 5, pp. 1326–1338. © Pleiades Publishing, Ltd., 2015.
Original Russian Text © N.N. Koval, Yu.F. Ivanov, I.V. Lopatin, Yu.H. Akhmadeev, V.V. Shugurov, O.V. Krysina, V.V. Denisov, 2013, published in Rossiiskii Khimicheskii Zhurnal, 2013, Vol. 57, Nos. 3–4, pp. 121–133.

Generation of Low-Temperature Gas Discharge Plasma in Large Vacuum Volumes for Plasma Chemical Processes

N. N. Koval, Yu. F. Ivanov, I. V. Lopatin, Yu. H. Akhmadeev, V. V. Shugurov, O. V. Krysina, and V. V. Denisov

Institute of High Current Electronics, Siberian Branch, Russian Academy of Sciences, pr. Akademicheskii 2/3, Tomsk, 634055 Russia
e-mail: koval@hcei.tsc.ru

Received January 1, 2013

Abstract—In the paper the principles of generation of low temperature capacitively coupled in a vacuum chamber of a large size with the use of original low-pressure arc discharges are considered. The designs of plasma sources and their main parameters are described. Examples of effective use of the generated plasma in plasma chemical modification of the surfaces of materials and products are presented.

DOI: 10.1134/S1070363215050485

INTRODUCTION

Low-pressure diffuse discharges burning both in the self-sustained and in the non-self-sustained regimes provide an efficient means for generation of low-temperature plasma in large vacuum chambers. Depending on the configuration of the electrode system, pressure of the working gas, and power supply of the discharge system, different types of discharges are distinguished: spark, glow, and arc discharges; transition modes are also possible, where discharges of different types are combined. The use of high-frequency (HF) and radiofrequency (RF) power supply, as well as external magnetic fields allow intensification of plasma formation at relatively low pressure.

In the present paper we consider the use of low-pressure arc discharges for efficient generation of plasma in fairly large (up to 1 m^3) vacuum chambers. Examples of automated setups, where such discharges are realized, are given and some applications of the generated plasma in plasma chemical processes, primarily in surface modification of materials and products, are described.

The main advantages of using arc discharges for plasma generation are as follows:

– high discharge currents (from several amperes to several kiloamperes), both in the continuous and in the pulse frequency regime, which allows generation of plasma with the charged particle density of 10^{15}–10^{17} cm^{-3} in large vacuum chambers at pressures of (0.1–1) Pa;

– low discharge voltages (tens of volts), which allows highly energy efficient plasma generation;

– wide range of control of plasma parameters both by varying discharge parameters and by varying the plasma-forming gas pressure;

– generation of a fairly uniform-density plasma (±20%) in the entire working volume which can reach a few cubic meters;

– possibility of completely automated generation of low-temperature gas discharge plasma.

All these main advantages are realized in the design of electronic-ionic-plasma equipment due to the use of specific self-sustained and non-self-sustained low-pressure arc discharges.

Plasma Generators on the Basis of a Non-Self-Sustained Hot Cathode arc Discharge

A hot cathode plasma source PINK was developed using a combined cathode comprising a hot and a hollow cathodes [1–4]. A simplified design and a picture of the PINK plasma generator on the basis of a non-self-sustained hot cathode arc discharge are presented in Fig. 1.

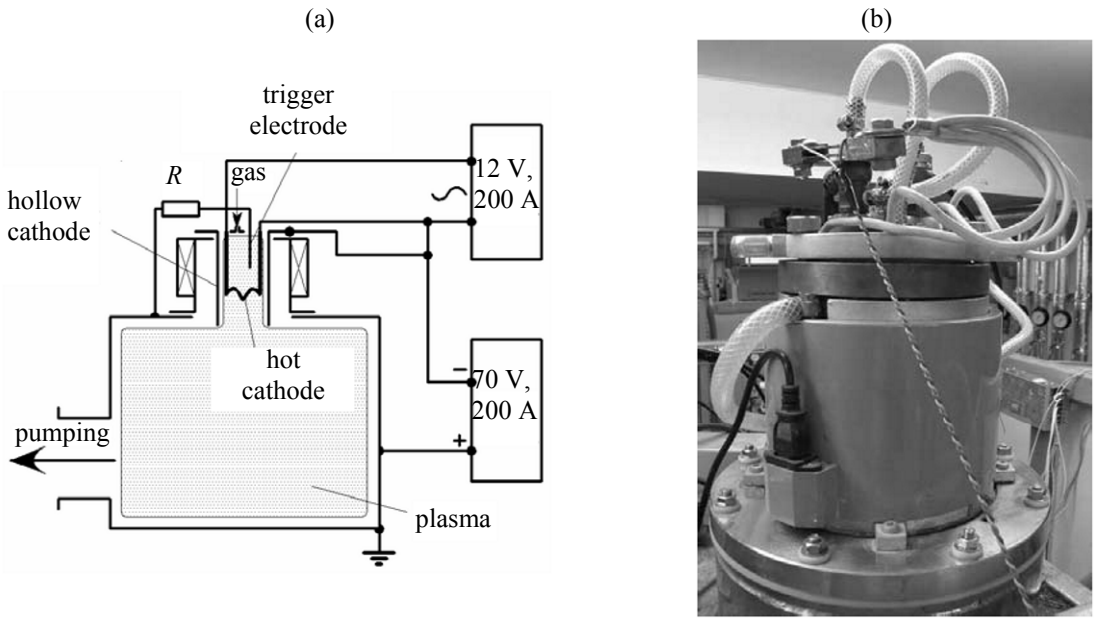

Fig. 1. (a) Schematics and (b) general view of a hot cathode plasma source.

Discharge is ignited when a longitudinal magnetic field (induction 0.1–3 mT) is created in the working volume of the plasma generator and the electrodes of the discharge system are powered. The electrons emitted by the hot cathode are accelerated toward the auxiliary electrode (which plays the role of an auxiliary anode in the moment of discharge ignition) and ionize gas in the cathode region, thereby inducing discharge ignitions in the hot cathode-ignition electrode gap. Therewith, the hollow cathode is filled with plasma which, due to the density gradient of charged particles, propagates into the vacuum chamber. As a result, discharge burning switches to the main anode whose role is fulfilled by the inner walls of the vacuum chamber, and in the ignition electrode circuit, there is a weak current (≤1 A). This stabilized the main discharge and prevents it from extinction if there are pressure fluctuations in the chamber. The external magnetic field imparts helical motion to the electrons emitted by the hot cathode, thereby prolonging their way to the anode and enhancing the ionization efficiency of gas. By varying the filament current and electron emission from the hot cathode one can vary the discharge current and realize a non-self-sustained arc discharge without cathode spot with a current of tens-to-hundreds of amperes at a discharge voltage of a few tens of volts. Therewith, the volume of the discharge chamber is filled by a gas plasma with the charged particle density of 10^{17} m^{-3} and the uniformity of no worse than ±15% from the mean value.

The voltage–current characteristic of the discharge in the PINK plasma generator has an ascending pattern as a result of that increasing discharge voltage increases the gas enhancement factor (increase in the number of charges particles). Increase of the filament current I_f increases the discharge current I_d and decreases the discharge voltage U_d (Fig. 2). Therewith, the hollow-cathode current I_{hc} also increases. Such a dependence pattern is associated with increasing electron emission from the hot cathode [6].

The discharge efficiently generates a low-temperature gas discharge plasma with a fairly high (up to

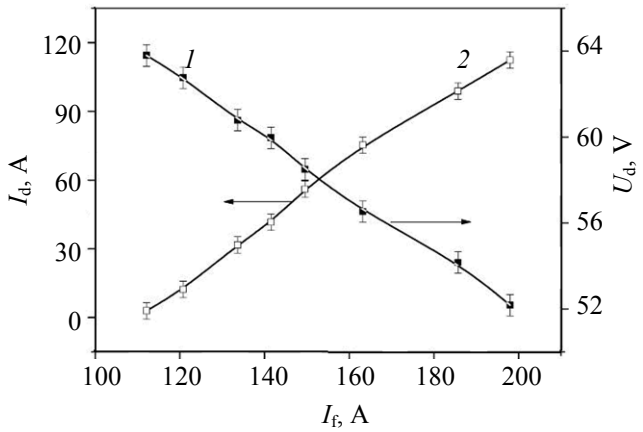

Fig. 2. Dependences of the (*1*) discharge voltage U_d and (*2*) discharge current I_d on the filament current I_f. Working gas nitrogen, pressure 1 Pa, magnetic field strength 2.1 mT.

10^{17} m^{-3}) density. Such plasma can provide purification and activation the surface of products, heating to a desired temperature, diffusion saturation of the surface of iron and titanium alloys with nitrogen, as well as plasma-ion assistance in electric arc discharge deposition of functional coatings [3].

The design of the PINK plasma generator was used to develop a series of hot cathode plasma generators PINK-P [5] with the active plasma zone up to 120 cm long.

The plasma generators have the same configuration and differ from each other only by the dimensions and number of hot cathode channels. Each channel consists of two hot cathodes and three current. Such design provides more stable operation of the plasma generator in time-consuming processes: if one of the hot cathodes has accidentally broken down, the system automatically switches to the second cathode without interrupting the technological process. By varying the number of hot cathode channels, the working length of the hollow cathode can be increased from 20 too 120 cm at steps of 20 cm. At present the plasma generators PINK-P0.4M, PINK-P0.6M, and PINK-P1.2M with the working lengths of the hollow cathode 40, 60, and 120 cm, respectively, have been developed, fabricated, and tested.

The plasma generators are powered from unified sources comprising the power units for discharge, magnetic coils, and hot cathodes, and the number of power sources depends on the number of the plasma generator. The discharge and magnetic-coil power units are combined in a single structure module. The discharge power unit is designed as a high-frequency inverter circuit and equipped with an automated system for protection from short-circuit currents and microarc discharges on the hollow cathode.

Plasma generators with a hot cathode have found a fairly wide application in chemical thermal surface treatment of metals and alloys [7]. The hot cathode allows the plasma density (charged particle density) to be increased at fairly low discharge voltages, and, therewith, the discharge current can be varied independently on the discharge voltage and the pressure in the working chamber. The discharge pressure in such systems varies from ~0.1 to ~1 Pa. This gives certain advantages regarding the free path of ions and electrons, specifically, increased free path of ions makes possible efficient ion purification of surfaces and thus exclude hydrogen-containing gases from the working mixture for steel Nitriding and accelerates the Nitriding process.

Gas Plasma Generator on the Basis of a Cold Hollow-Cathode arc Discharge

The technology of plasma generation with the use of a hot cathode as an ionization source has some drawbacks which can be overcome using different types of discharge, for example, a vacuum arc discharge. At the same time, with the vacuum arc discharge as an ionization source a problem of cathode erosion associated with the presence of a cathode surface spot; as a result, the plasma flux contains, along with ions, metal macroparticles (microdroplets) released from the cathode surface. Cathode erosion products are deposited on the surface and form a metal-containing layer which prevents nitrogen diffusion into the depth of the substrate. To overcome this drawback, we suggested a technique for the generation of gas-discharge plasma on the basis of arc discharge with a cathode spot with separation of the vacuum arc plasma flux from macroparticles.

This technique was realized in a plasma source with an integral cold hollow cathode with a diaphragm (PIPK) [8, 9] (Fig. 3). The characteristic dimensions of the plasma source are as follows: inner diameter of the hollow cathode D = 110 mm, hollow-cathode length L = 200 mm, and outlet diaphragm diameter d = 55 mm.

When pulsed voltage is applied ($U_{pulse} \approx 12$ kV, $t_{pulse} \approx 500$ μs, $I_{pulse} \approx 200$ A), a breakdown of the surface of the dielectric separating the trigger electrodes takes place to form a cathode spot on the inner surface of the cathode, which generates a primary plasma. The anode potential propagates to the cathode hollow, and a self-sustained steady-state arc is ignited between the hollow anode (working chamber) and the hollow cathode. The cathode spot moves along the inner surface of the hollow cathode. The motion path goes close to the maximum of the magnetic field created by a short magnetic coil. The transmission sputtering of the cathode material to the opposite (with respect to the immediate position of the cathode spot) side of the cathode hollow prolongs the service life of the latter and prevents penetration of the sputtered material to the anode hollow.

Such plasma source can be used generate plasma of active gases, for example, oxygen. The plasma source with a hot cathode is hardly suitable in this case, because oxygen actively oxidizes the hot cathode

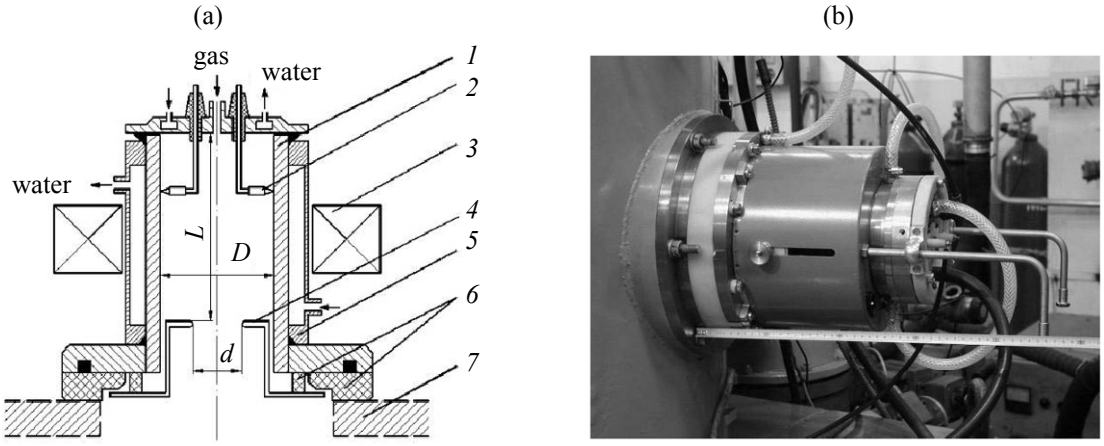

Fig. 3. (a) Schematics and (b) general view of a cold hollow-cathode plasma source: (*1*) hollow cylindrical cathode; (*2*) trigger; (*3*) short magnetic coil; (*4*) arc quencher; (*5*) cylindrical cathode cooling jacket; (*6*) insulator; and (*7*) vacuum chamber (hollow anode).

(temperature up to ~2800 K), and its service life decreases to 1–2 h, and the discharge parameters are unstable throughout all this time.

Under the condition of constant pressure of 0.44 Pa and magnetic field of 0.6–14 mT, the discharge voltage is almost independent on the discharge current [9]. In an argon atmosphere, the arc is sustained at a low voltage (U_d = 22–24 V). In the working pressure range 0.08–0.8 Pa, the discharge voltage varies no more than 10%, i.e. the voltage–current dependences are linear and slightly ascending.

The service life of the cathode in the described plasma generator is longer than 100 h, whereas that in the hot cathode plasma generator PINK is no longer than 24 h. The weight-and-dimensional parameters of the two plasma generators are virtually the same, which makes these apparatuses interchangeable.

Metal Plasma Generators on the Basis of arc Discharge with a Cathode Spot

Metal plasmas generated by means of a low-pressure arc discharge with a cathode spot are used for manufacturing metal coatings. This technology started to be vigorously developed in 1979s [10], while beginning in 1980s the USSR initiated mass production of evaporators like Bulat, NNV-6, etc. The main building blocks of such apparatuses are electric arc evaporators with a cold cathode [11]. Such electric arc evaporators form the operational basis of many up-to-date metal plasma sources. The cathode arc evaporator can be operated at discharge currents of up to 150 A, which ensures high evaporation rates (up to 5 μm/h).

Standard arc evaporators (Bulat, NNV-6) have a number of drawbacks. First, because of the design features, the surface area of the cold part of the working cathode comprises no more than 30% of the rare side of the cathode. Insufficient heat removal, especially at high discharge currents, may lead to local overheating of the cathode surface along the motion path of the cathode spot and, in the long run, increase the integral temperature of the cathode. In its turn, this increases the droplet fraction in the plasma flux. Furthermore, such apparatuses do not allow large-volume cathodes (>175 cm^3) because of the possible vacuum seal failure. Second, the shape of the cathode holder allows only direct water cooling, which makes impossible the use of cathodes from porous materials, such as silumin, or materials obtained by self-propagating high-temperature synthesis.

We developed a new arc evaporator (temporary name DI-100) which, due to a changed construction of the cathode assembly, is almost free of the main drawbacks of standard arc evaporators. The improved cooling allowed the integral temperature of the cathode to be decreased due to vacuum arc evaporation, which, in its turn, halves the droplet fraction in the plasma flux (Ti coating deposition). One more constructive feature of the DI-100 arc evaporator is that allows porous evaporating cathodes. A copper diagram (thickness 0.5 mm) is mounted between the evaporating cathode and its water cooling system, which ensures a fairly efficient cooling by preventing direct contact of the cooling water and the cathode.

DI-100 is designed for the technologies of synthesis of metal and composite coatings. The working cathode

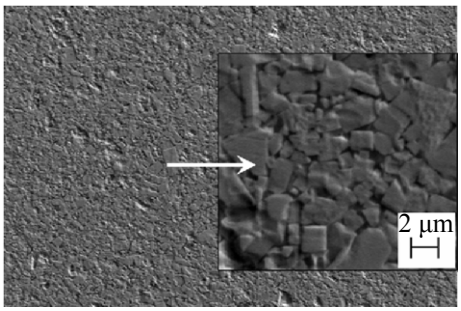

Fig. 4. Transmission electron microscopic image of the VK-8 alloy surface after treatment in an arc discharge plasma. Working gas argon; p = 0.3 Pa; I_d = 20 A; U_d = –1000 V.

is 100 mm in diameter and 50–60 mm in height, i.e. it is 2–4 times larger compared with the cathode for NNV-6 and Bulat. The maximum current discharge is increased to 250 A. This allows the coating growth rates to be increased to 20 μm/h, which is 1.5–2 times higher compared to a standard plasma source (NNV-6); therewith, the coating uniformity is only slightly (15–20%) sacrificed within the scattering angle of the plasma flux.

Plasma Surface Treatment of Materials

Reactive Ion Plasma Etching of the Surface of Metal-Containing Materials

Reactive ion plasma (RIP) etching can be used to explore the surface structure of a material, remove layes of desired thickness and shape at the stage of complex processing, for example, to remove oxide inclusions and adsorbed gases from the surface layer, to heat and activate the surface before nitrogentaion or deposition of functional coatings.

Figure 4 shows a characteristic image of the surface of a hard tungsten alloy VK-8 (WC+8%Co) after RIP treatment, illustrating etching of the cobalt binder at tungsten carbide grain boundaries and enhancing surface roughness (Table 1). By contrast, the surface roughness of 12H18N10T steel samples does not enhance as the plasma density is increased from 1.0 × 10^{16} to 5.2 × 10^{16} m^{-3} and the density of the ion current to the substrate is increased from 15 to 20 A/m^2 (see Table 1).

The rougness of the 12H18N10T (0.12% C; 18% Cr; 10% Ni; 0.8% Ti) steel surface scarcely varies with substrate potential. The etching rate increases to 0.64 μm/h at the shift voltage of –1000 V (Table 2). In the case of a hard tungsten alloy, increasing shift voltage increases the etching rate and surface roughness (see Table 2). It is worth noting that an increase of the arc discharge current and negative shift potential increases the ion current density and, as a result, the substrate temperature, which, too, may affect the etching rate.

Table 1. Surface roughness R_a and etching rate v_e of steel and tungsten alloy as a function of arc discharge current and gas plasma density

I_d, A	j_i, A/m^2	n, 10^{16}, m^{-3}	T, °C	12H18N10T steel		VK-8 alloy	
				R_a, μm	v_e, μm/h	R_a, μm	v_e μm/h
20	1.5	1.0	140	0.15	0.26	0.22	0.41
50	1.8	2.7	214	0.12	0.36	0.34	0.45
90	2.0	5.2	315	0.16	0.33	0.62	0.89

Table 2. Surface roughness and etching rate of steel and tungsten alloy as a function of shift voltage U_1 (I_d = 20 A, n = 1 × 10^{16} m^{-3})

U_b, V	j_i, A/m^2	T, °C	12H18N10T steel		VK-8 alloy	
			R_a, μm	v_e, μm/h	R_a, μm	v_e, μm/h
200	0.5	55	0.13	–	0.14	–
400	1.0	75	0.13	–	0.22	–
600	1.5	140	0.15	0.26	0.22	0.41
1000	2.5	232	0.14	0.64	0.34	0.58

Thus, by varying the discharge current in the PINK source without varying the working gas pressure one can control the plasma density and, consequently, the ion current density to the substrate, thereby controlling the RIP surface etching of materials.

Etching using a hot cathode plasma source (PINK) in argon, as well as a cold hollow cathode plasma source (PIPK) in an argon–oxygen mixture was used to remove a worked-out diamond-like carbon coating from the surface of a hard alloy cutting tool. A capacitive plasma was generated in a vacuum chamber, a negative shift potential was applied to WC−Co hard allow samples, and etching was performed. The etching rate of the diamond-like carbon coating at an argon pressure of 0.4 Pa, PINK discharge current of 60 A, and shift potential of –1000 V was ~1.3 μm/h. Therewith, the etching rate of uncoated parts of the hard alloy was as high as 2.8 μm/h, which led to deposition of a WC−Co layer on the surface of the diamond-like carbon coating. To avoid this effect, etching was performed in oxygen using the cold hollow-cathode plasma source PIPK. To improve the performance of the plasma source and increase the ionization degree, a 10:1 mixture of oxygen and argon was used. The etching rate of the diamond-like carbon coating at a gas pressure of 0.4 Pa, PIPK discharge current of 75 A, and shift potential of –1000 V was 1.7 μm/h, while the etching rate of the WC−Co hard alloy was as low as 0.4 μm/h.

Nitriding of Construction Steel in a Low-Pressure arc Discharge Plasma

Nitriding of construction and tool steels with the aim to enhance their corrosion resistance and microhardness is widely used in machine building [12–15]. Ion nitriding is most commonly performed using glow discharge which, along with undeniable advantages (stably ignited and sustained in a low vacuum, 100–500 Pa, and easily generated in large volumes), has certain disadvantages: high discharge voltage and, as a result, high power consumption; long process time and necessity to introduce hydrogen for binding oxygen which is present in the discharge chamber at a high gas pressure.

Had conditions been created that exclude oxide formation in the process of saturation of the surface of steel items with nitrogen [16], it would have proved possible to, on the one hand, accelerate the nitriding process and, on the other, no longer introduce hydrogen [17] to the vacuum chamber.

Table 3. Thickness of the nitride and diffusion layers as a fiunction of nitriding time

Time, min	Layer thickness, μm	
	nitride Fe_4N	diffusion
10	3–4	90
20	4–6	170
40	7–9	200
60	8–10	220
120	10–12	260
300	10–12	320

Below we present the results of research on revealing the regularities of steel nitriding and optimizing the conditions of nitriding in a low-pressure arc discharge plasma.

Steels 45 (0.45% C) and 40H (0.4% C; 1.0% Cr) (samples 20 mm in diameter and 10 mm in height, mechanically polished and purified by ultrasonication) were used. Nitriding was performed in a hot cathode arc discharge plasma [4] (dicharge current I_d = 50 A, discharge voltage 40 V, pressure 0.3 Pa). Plasma with the charged particle density of 10^{16} m^{-3} was generated in a chamber 0.2 m^3 in volume. The sample was placed into the chamber and powered with a negative shift voltage of up to –1000 V. Therewith, a layer of spatial charge formed around the sample. At a low working-gas pressure (0.1 Pa) the plasma ions reaching the sample surface were accelerated in this layer to the energy corresponding to the applied voltage.

It was found that the first layer formed as a result of nitriding (I_d = 50 A, U_{shift} = –600 V, 5 h) on the sample surface is a continuous γ-phase (Fe_4N nitride) with the Brinell hardness 7.5–8 GPa. The first layer is gradually changed to the second, α-phase layer (a solid solution of nitrogen in ferrite), whose hardness varies from 6.5 to 2.5 GPa (core hardness) within the sample depth of 300 μm. The total thickness of the nitrided (diffuse) layer unsteadily increases with nitriding time (Table 3). Initially, the γ- and α-phases are formed at a high rate and then both processes slow down.

In the considered process, at a pressure of 0.1 Pa, the ions with a fairly high (estimated) energy of 600 eV bombard the sample surface and spuuter the oxide film which would otherwise hinder the nitridung

process; this eliminates the necessity to introduce hydrogen into the discharge chambed for binding residual oxygen. Compared to the nitrided layer obtained in glow discharge, the thickness of the Fe_4N layer formed in arc discharge is, at the same temperature and treatment time, 2–3 times larger, which is most probably explained by a higher plasma density of high-energy ions bombarding the sample surface.

In the next experimental series we studied ferrite–perlite (annealed) and martensitic (hardened) steels 40H and 18H2N4A (0.14%C, 2.3%Cr, 3.8% Ni). The diffusion nitrogen saturation of steel 40H in a low-pressure vacuum arc discharge plasma was performed at ~200°C (averaged over the sample) for 2, 4, 6, and 8 h; steel 18H2N4A was treated at 530°C for 2 h.

The nitriding of a hardened steel 40H for 2 h resulted in a change in the defect substructure of a ~1-μm surface layer, i.e. decrease in the scalar dislocation density, formation of subgrains (centers) of dynamic recrystallization, and destruction of massive martensite crystal boundaries. Moreover, a change in the phase composition of the steel was also observed, specifically, formation of $Fe_4[Fe(CN)_6]_3$ iron carbo-nitride particles in the bulk and along the martensite crystal boundaries of and in their junctions, and also formayion of $Fe_{16}N_2$ iron nitride particles in the bulk of the martensite plates and γ-Fe_4N particles in the near-boundary volumes of dynamic recrystallization centers. After 8-h nitriding, a multilayer structure is formed, which comprises (from top to bottom) a thin (~1 μm) surface layer (presumably, γ-Fe_4N) followed and , a nanocrystalline layer with the crystallite size ~30 nm, a noncrystalline layer with the crystallite size ~10 nm, a martensite structure including dynamic recrystallization subgrains, and, tempered martensite structure. The the depth of ~5 μm a structure similar to the starting structure is present.

At a higher nitriding temperature, a hardened steel (steel 18H2N4A, 530°C, 2 h) undergoes more essential changes in the defect substructure (decrease in the scalar dislocation density, fragmentation and partial destruction of martensite crystal boundaries, initiation of recrystallization) and phase composition of the surface layer (formation of ε-Fe_2N iron nitride particles).

At a 3–5 μm depth from the nitrided surface, the steel substructure is represented by α-phase grains and subgrains (≈0.45 of the structure) and massive martensite. Extended interlayers of the second phase ($Fe_4[Fe(CN)_6]_3$ and ε-Fe_2N) are formed along the martensite crystal boudaries and subgrains.

Thus, we obtained evidence to show that nitriding at ~200 C in a low-pressure gas discharge plasma makes it possible to modify the surface layer of a hardened steel (steel 40H) without affecting the structure of the bulk material. The multilayer structure of the modified layer reflects consecutive trans-formation of the structural and phase composition of the steel in the course of nitriding. Analysis of the evolution of the defect substructure of martensite crystals allows us to suggest that the diffusion nitrogen saturation in a low-pressure gas discharge plasma can be used not only to form protective surface layers, but also to stabilize the defect substructure of the surface volume of a material.

The nitriding of an annealed steel 40H (200°C, 2 h) results in formation of $Fe_{2\text{-}3}N$ and γ-Fe_4N iron nitride particles in the surface layer. The particles have a round shape, and their average size is 10–20 nm. In structurally free ferrite grains the particles reside on dislocations, and in the ferrite interlayes of laminar perlite colonies they form mutually parallel lines along the {110} α-Fe direction. The line-to-line distance is 25–40 nm. The formation of such a periodic structure can be explained by the presence of a periodically changing field of elastic stresses in the ferrite plates. The reason for the development of this field is a periodic defect structure of cementite/ferrite interfaces. The trasformation of cementite plates is accompanied by their fragmentation and formation of $Fe_{20}C_9$ and Fe_2C carbides along the cementite/ferrite interfaces. The latter is evidence for the destruction of cementite plates during low-temperature nitriding.

In the layer located at a depth of 1…2 μm, nitriding leads to a considerable increase of the scalar dislocation density in structurally free ferrite grains and perlite grains and destruction of cementite plates to form $Fe_{20}C_9$ nanoparticles in laminar perlite grains.

Increased nitriding temperature of an annealed steel (steel 18H2N4A, 530°C, 2 h) results, first of all, in a complete transformation of the defect substructure of the material bulk immediately adjacent to the nitrided layer (foil, thickness ~0.2 μm). A subgrain (subinter-face) structure (subgrain size ~0.2 μm) is formed in the bulk of laminar perlite grains. Globular cementite particles are situated along subgrain boundaries. In the bulk of ferrite grains a structure with a high density of flexural extinction contours is formed, implying a high

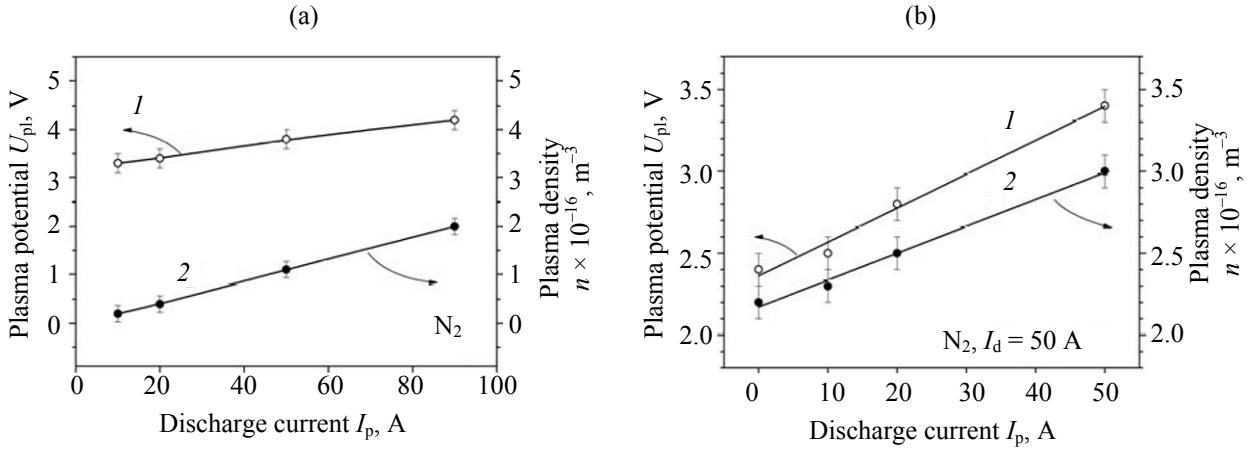

Fig. 5. Dependences of the plasma (*1*) potential and (*2*) density on PINK discharge current: (a) nitrogen plasma and (b) gas metal plasma. Working gas nitrogen.

twist curvature of vrystal lattice the material, as well as the presence of γ-Fe_4N.

Gas–Metal Plasma-Assisted Deposition of Multicomponent Functional Coatings

Using an additional plasma source on the basis of a non-self-sustained arc discharge with a combined hot and hollow cathode (PINK) is rational in vacuum arc plasma−assisted deposition of coatings [3]. First, PINK allows coatings to be deposited at a low pressure (~0.1 Pa) and, as a result, they contain almost no gas inclusions, i.e., have a denser texture. Second, continuous bombardment of the growing coating with low-energy working gas ions allows removal of adsorbed gas from the surface and refinement of the coating structure. Third, the presence in the vacuum discharge chamber of additional ions generated by the hot cathode plasma source ensures maintaining arc discharge at low currents (<20 A). Fourth, combined use of a plasma source and a system for supply of a negative shift voltage to the substrate with a growing coating allows one to decrease considerably the fraction of the droplet phase and thus approach one of the main problem of the vacuum arc deposition technology. The droplet fraction in the mixed gas−metal plasma generated by low-pressure arc discharge is decreased due to the reflection of macro-particles negatively charged to the floating potential (–6 to –8 V) in the arc gas discharge plasma (electron gas temperature $T_e \approx 5-7$ eV) from the sample powered with a negative supply voltage (–100 V) [18, 19].

Studying cathode spots in the course of vacuum cathodic arc evaporation by means of a high-resolution CCD camera showed that preliminary gas ionization in the non-self-sustained arc discharge mode by means of a hot cathode plasma source has no effect on the evolution of the number of cathode spots and their associations with increasing arc discharge current and the motion rate of a single spot. No appreciable effect of working gas ionization on cathode erosion in vacuum arc evaporation and on the rate of coating growth was detected within measurement error.

The results of study on the effect of the discharge current of the plasma source on the parameters of the gas–metal mixed plasma in a nitrogen medium are presented in Fig. 5.

The average electron temperature in the gas and mixed plasmas were ≈1.4 and 0.9–1.0 eV, respectively.

Analysis of the dependences in Fig. 5 shows that the density of the gas–metal plasma is roughly equal to the sum of the densities of the gas and metal plasmas, measured at the same parameters of arc discharges. An increase of the discharge current in the PINK source at a constant pressure of the working gas increases the plasma density. If the sources of metal (electric arc evaporator) and gas discharge plasmas work simultaneously, an increase of the discharge current in the PINK source at a constant arc discharge current leads to a parallel increase in the density of the mixed plasma. Thus fact suggests that by varying PINK discharge current (at a constant pressure in the discharge chamber) one can control the density of the ion flux to the substrate, thereby varying the stoichiometry of the growing coating. This makes it possible to simplify the technology of production of

Table 4. Characteristics of coatings formed by vacuum arc evaporation of Ti–Cu, Ti–Si, and Ti–Al composite cathodes[a]

Coatinge	n, at %		d_{av}, nm	HV, GPa	E, GPa	ε_{min}, %	$L_{c,max}$, N	μ_{min}
	EDA	XRF						
TiN	–	–	~100	20–25	300–350	~75	3.6	0.40
Ti–Cu–N	~2	~12	18	38–42	350–400	~50	10.7	0.22
Ti–Si–N	–	~2	7	34–52	400–800	~20	5.8	0.41
Ti–Al–N	~20	–	5–6	31–40	450–650	~35	3.6	0.23

[a] (n) Concentration of the dopant element in the coating as determined by the energy dispersion (EDA) and X-ray fluorescent analysis (XRF); (d_{av}) average diameter of crystallites of the main phase; (HV) hardness; (E) Young modulus; (ε_{min}) residual deformation; ($L_{c,max}$) critical load; and (μ_{min}) friction coefficient.

multilayer and gradient coatings and improve the reproducibility of deposition of such functional coatings more reproducible.

Synthesis of Multilayer Hard and Superhard Coatings

Vacuum arc coating deposition is most commonly performed as multistage process is a single vacuum cycle. The first stage involves purification, heating, and activation of the sample surface by metal-ions or working gas ions. The second stage may involve the deposition of an auxiliary sublayer for improving adhesion of the target coating to the substrate. The target coating is synthesized at the third stage. The final stage may involve cooling of coated samples.

In the case of vacuum arc plasma-assisted deposition, the first stage (purification, heating, and activation of the surface) is performed using a low-pressure non-self-sustained discharge plasma. Note that when the gas discharge plasma is generated at low working pressures (0.01–0.1 Pa), the mean free path of ions is longer than the characteristic thickness of the spatial charge layer formed at the substrate powdered by a negative shift voltage. As the negative shift voltage is varied, the ions that reach the substrate surface having passed through the spatial charge layer formed at the substrate at a low pressure are accelerated to an energy corresponding to the applied voltage (the energy loss due to collisions with other particles can be neglected). Thus, working gas ions with the energy ~100–1000 eV can be used to success to purify the surface by etching a thin surface layer (oxide films, adsorbed gases) not affecting the initial structure, as well as to prepare the surface (heating and activation) for the subsequent ion plasma processes (nitriding, coating deposition).

The vacuum arc synthesis of coatings at the second and third stages is performed in the plasma-assisted mode at a relatively low pressure (~0.1 Pa). Therewith, as mentioned above, a dense coating (containing no gas inclusions) is formed, and continuous bombardment of the growing coating by low-energy ions of the working gas removes the adsorbed gas from the surface and refines the structure of the growing coating.

It should be noted that a specific combination of deposition parameters is required to obtain a close-to-stoichiometric coating. Thus, titanium cathode evaporation to obtain a TiN coating is performed at the arc discharge evaporator current 50–100 A, nitrogen pressure ~0.1 Pa, and shift voltage–(100–300) V on substrates located at a distance of 300 mm from the exit aperture of the evaporator; coating growth rate 2–3 μm/h.

One of the promising applications of the vacuum arc deposition technology is manufacturing coatings with the crystallite size no more than 100 nm. Such coatings characteristically combine superhardness (Vickers hardness ≥40 GPa), high durability, resistance to oxidation, etc. Experiments on electric arc plasma-assisted deposition showed that the crystallite size is smaller if the coating contains small amounts of alloying components (Cu, C, Si, Al) which prevents coalescence of crystal nuclei, thereby suppressing growth of grains of the main coating material [20, 21]. First publications on the use of chemical vapor deposition (CVD) processes [22] and magnetron sputtering [23] appeared in late 1990s. At present the processes of formation of such multicomponent plasma coatings as Ti–Si–N, Ti–Al–N, Zr–Cu–N, Ti–Si–Al–N [24–27], and others are under intensive research.

Table 4 lists the characteristics of the nitride coatings synthesized on metal substrates by the evaporation of Ti–Cu, Ti–Si, and Ti–Al composite cathodes in a nitrogen plasma.

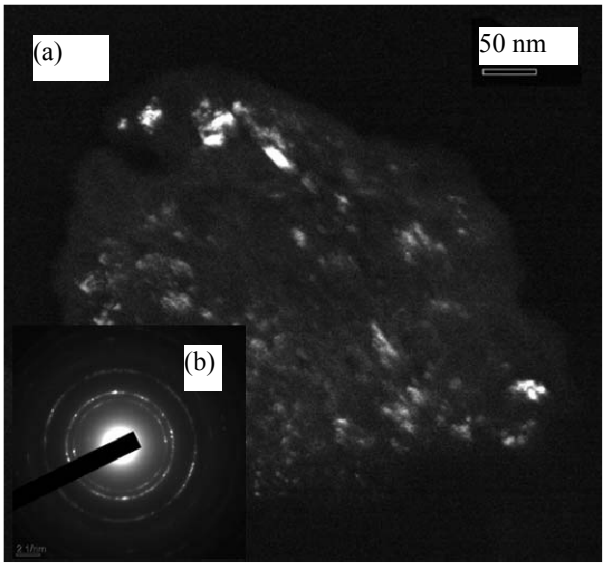

Fig. 6. Electron microscopic image of the Ti–Si–N coating structure: (a) dark field obtained in a {111} TiN ring reflex and (b) microelectronogram.

The three-component coatings all have a nanocrystalline structure (Fig. 6). The main phase is d-TiN with the mean crystallite size less than 20 nm. The dopant concentrations in the coating and evaporated cathode are the same if the dopant is a metal (Cu, Al). The concentration of silicon in the Ti–Si–N coating is 5 times lower than its concentration in the cathode.

Nanocrystalline multicomponent coatings are 1.5–2.5 times harder than the TiN coating, and, when deposited in optimal conditions, they become superhard (≥40 GPa). The highest residual deformation was found in the TiN coating and the lowest, in the Ti–Si–N coating. The elastic relaxation of coatings formed by powder cathode evaporation is 2–3 times higher compared to TiN coatings.

The Young moduli of multicomponent coatings span the range 350–800 GPa. The best adhesion to metal substrates is characteristic of Ti–Cu–N coatings: they start to destroy, when the critical load on the indenter is 10.7 N, which is 3 times as high as that for the TiN coating on a hard alloy substrate. The lowest friction coefficients are in copper- or aluminum-doped coatings (≤0.2), which points to enhanced durability of such coatings.

Apparatuses for Complex Ion Plasma Treatment of Items

Combining different plasma methods for surface modification allows considerable improvement of consumptive qualities of the treated items and optimization of characteristics of the modified surfaces. With the aim to combine different methods of ion plasma treatment in a single process cycle, the Institute of High Current Electronics, Siberian Branch, Russian Academy of Sciences, has developed special-purpose process apparatuses DUET, TRIO, and QUADRO [28, 29]. These apparatuses allow realization in a single process cycle, a series of consecutive operations of treatment of materials and items, specifically, preliminary heating and degassing, ion purification, etching, and activation of the surface with arc plasma; chemical thermal treatment (nitriding) for forming on the surface on an item being treated of a diffusion of layer by means of a low-pressure non-self-sustained arc discharge plasma; as well as electric arc plasma-assisted deposition of mono- and multilayer surephard (>40 GPa) nanocrystalline coatings on the basis of several pure metals or their compounds (nitrides, carbonitrides, or carbides).

Fig. 7. General view of the DUET apparatus.

The main applications of the DUET, TRIO, and QUADRO apparatuses include hardening of cutting tools from high-speed steel and hard alloys, die tools, press forms, and other details of machines and mechanisms and deposition of their surface of metal and composite superhard nanostructured coatings.

DUET Apparatus (Fig. 7)

The apparatus is equipped with two hot cathode plasma sources (PINK) for generation of capacitive arc gas discharge plasma and a DI-100 cathodic arc evaporator for deposition of hardening coatings (TiN, CrN). The plasma sources can be operated both independently and concurrently (“duet” operation).

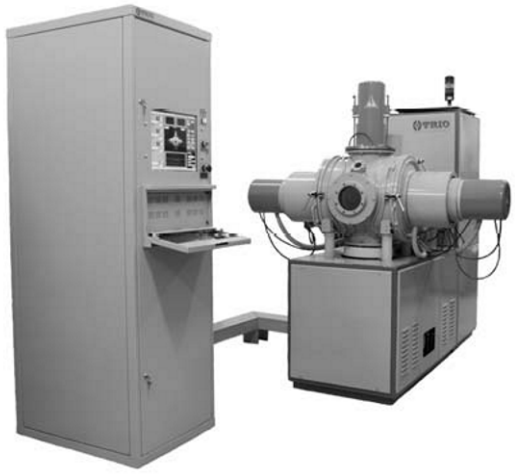

Fig. 8. General view of the TRIO apparatus.

The DUET apparatus comprises a vacuum chamber, a vacuum system, a gas supply system, a water cooling system, a power supply system, and a control system with automation units. The automated control system comprises two modules: engineering and vacuum. It ensures safe operation and automated vacuum pumping. The system is designed as a separate block and consists of two controllers, each responsible for its module: engineering and vacuum.

The working chamber is fabricated from a stainless steel (inner dimensions 750 × 750 × 750 mm). The PINK plasma source is mounted on the top flange of the chamber and the cathodic arc evaporator, on the side flange. The tools to be treated are placed into separate wells in a table fixed on a rotary shaft inside the working chamber. The walls of the chamber, manipulation shaft, and housings of the plasma sources are equipped with water cooling systems with an automatically controlled water supply. Automatic evacuation of the chamber is performed by means of a turbomolecular pump (limiting pressure 10^{-3} Pa).

A negative shift voltage is supplied to details or items to be treated either from low-voltage (up to –300 V) or high-voltage (up to –1500 V) continuously controlled power sources equipped with a system for electric arc suppression and prevention of sustaining microarcs on the surface of the treated items. The power sources are controlled manually. The power source of the PINK plasma source is equipped with a system which prevents transition of the discharge to the cathode spot mode.

The working gases are argon and nitrogen.

DUET is used for working out new regimes of electric arc plasma-assisted deposition of functional coatings.

TRIO Apparatus (Fig. 8)

The TRIO apparatus comprises a hot cathode plasma source (PINK) to generate capacitive arc discharge plasma with a non-self-sustained arc current of up to 200 A without cathode spot and two arc evaporators with a current of up to 150 A, which serve for evaporation of the cathode material and deposition of functional coatings. Plasma generators can be operated both independently and concurrently. The apparatus consists of a vacuum chamber, a vacuum system, a gas supply system, a water cooling system, a power supply system, and an automated control system.

The main executive unit of the automated control system is an ADAM-5000 commercial controller. The components of the system are controlled by both discrete and analog signals.

The water-cooled vacuum chamber is designed as a horizontal cylindrical vessel (diameter 500 mm, length 500 mm) with two side engineering doors. The side doors, as well as the top of the chamber have flanges for mounting plasma sources.

The working chamber is evacuated by means of two sliding vane rotary pumps and one turbomolecular pump. The working gas supply system comprises automatic inlet valves with built-it electronic control blocks. Nitrogen, argon, or other gases can be used as working gases, depending on the task. Gases can be supplied individually or as a mixture with a desired composition. The source of the negative shift voltage applied to the items to be treated allows varying the voltage (0–1000 V), pulse repetition frequency (2–40 kHz), and pulse duty factor (10–90%), providing the mean current of up to 10 A.

The automated control system of the TRIO apparatus implements automated pumping by a preset algorithm (manual control is also possible). A two-level system of protection (software and hardware) from pressure fluctuations and failures in water cooling system and commutation sequence of executive units is envisioned. The processes are controlled both manually and automatically, and the working parameters of each engineering unit can be set independently.

The TRIO apparatus is designed for treatment of small batches of commercial details and items, specifically, tools.

Fig. 9. General view of the QUADRO apparatus.

The QUADRO Apparatus (Fig. 9)

The QUADRO apparatus comprises the hot cathode plasma source PINK to generate capacitive arc discharge plasma with a non-self-sustained arc current of up to 200 A without cathode spot, the gas discharge source PIPK (plasma source with a cold hollow cathode) [6], which provides the cathode spot arc current of up to 250 A, as well as two arc evaporators with a current of up to 150 A, which serve for evaporation of the cathode materials and deposition of functional coatings. The other components are the same as in the TRIO apparatus (working vacuum chamber, vacuum system, gas supply system, water cooling system, power supply system, and automated control).

In terms of the design and functioning of the automated control system, QUADRO is similar to TRIO.

The working vacuum chamber is designed as a vertical cylindrical vessel with a side door. The top and side walls of the chamber, as well as the door have flanges for mounting plasma sources. The working chamber is automatically evacuated with a turbo-molecular pump (residual pressure up to 0.001 Pa). The chamber walls, manipulation shaft, and housings of the plasma sources are equipped with water cooling systems with an automatically controlled water supply.

The source of the negative shift voltage applied to the items to be treated allows varying the voltage, pulse repetition frequency, and pulse duty factor. Moreover, there is the possibility to supply a constant shift voltage with a special scheme for quenching electric microarcs arising in insufficiently clear surfaces of materials and items. Gas distribution and pressure stabilization are performed by an automated system comprising distributive valves and piezoelectric flow rate controller. The gas supply system is three-channel, and it allows setting the relative percent gas flow rates.

The infrared temperature-controlled heating is performed by means of two tubular electric heaters located at the bottom of the vacuum chamber.

The QUADRO apparatus is designed for complex surface modification of materials and items, including final surface purification and activation, electric arc nitriding, electric arc plasma-assisted deposition of mono- and multilayer coatings.

CONCLUSIONS

Research on the principal characteristics of the specific forms of self-sustained and non-self-sustained low-pressure arc discharges resulted in the development of a new class of efficient plasma sources for generation of a uniform low-temperature plasma in large vacuum volumes (≥ 0.5 m^3) at a pressure of 0.1–1 Pa (plasma density 10^{15}–10^{17} m^{-3}). The generated low-pressure arc discharge plasma can be used for surface purification and activation of materials placed in plasma and bombarded by plasma ions, for performing chemical thermal processes, in particular, metal nitriding with the aim to enhance the mechanical durability and corrosion resistance of the surface of details and tolls, for electric arc plasma–assisted deposition of functional coatings on the surface of materials and items, and for improving the decorative, wear-proof, and other useful properties of surfaces, materials, and items.

The described electric arc systems allowed development of DUET, TRIO, and QUADRO vacuum apparatuses for complex surface modification of materials and items, which make it possible to perform in a single vacuum cycle a series of consecutive engineering operations: final surface purification and activation, electric arc nitriding, oxidation , or nitrocarbiding with subsequent electric arc plasma–assisted deposition of mono- and multilayer superhard nanocrystalline multifunctional coatings.

ACKNOWLEDGMENTS

The work was financially supported in part the Russian Foundation for Basic Research (project nos.

13-08-98108-r-sibir' and 11-08-00453-a) and the Presidium of the Russian Academy of Science (program no. 24).

REFERENCES

1. Borisov, D.P., Koval, N.N., and Shchanin, P.M., *Izv. Vyssh. Uchebn. Zaved., Fiz*., 1994, no. 3, pp. 115–120.
2. RF Patent no. 2116707, 27.07.1998.
3. Borisov, D.P., Goncharenko, I.M., Koval, N.N., and Schanin, P.M., *IEEE Trans. Plasma Sci*., 1998, vol. 26, no. 6, pp. 1680–1684.
4. Shchanin, P.M., Koval, N.N., Goncharenko, I.M., and Grigor'ev, S.V., *Fiz. Khim. Obrab. Mater*., 2001, no. 3, pp. 16–19.
5. Shugurov, V.V., *Proc. 9th Int. Conf. on Modification of Materials with Particle Beams and Plasma Flows*, Tomsk, Russia, September 21–26, 2008, pp. 27–30.
6. Vintizenko, L.G., Grigoriev, S.V., Koval, N.N., et al., *Izv. Vyssh. Uchebn. Zaved., Fiz*., 2001, no. 9, pp. 28–43.
7. Meletis, E.I., *Surf. Coat. Technol*., 2002, vol. 149, nos. 2–3, pp. 95–113.
8. Schanin, P.M., Koval, N.N., Akhmadeev, Yu.Kh. and Grigoriev, S.V., *Technical Phys.*, 2004, vol. 49, no. 5, pp. 545–550.
9. Akhmadeev, Yu.H., Grigoriev, S.V., Koval, N.N., and Schanin, P.M., *Laser Part. Beams*, 2003, no. 21, pp. 249–254.
10. Aksenov, I.I., Belous, V.A., Padalka, V.G., and Khoroshikh, V.M., *Fiz. Plazmy*, 1978, no. 4, pp. 758–761.
11. GB Patent no. 1342560, 03.01.1974.
12. Lakhtin, Yu.M. and Kogan, Ya.D., *Struktura i prochnost' azotirovannykh splavov* (Structure and Strength of Nitrided Alloys), Moscow: Metallurgiya, 1982.
13. Arzamasov, B.N., Bratukhin, A.G., Eliseev, Yu.S., and Panaioti, T.A., *Ionnaya khimiko-termicheskaya obrabotka splavov* (Chemical Thermal Ion Treatment of Alloys), Moscow: MGTU im. N.E. Baumana, 1999.
14. Panaioti, T.A., *Fiz. Khim. Obrab. Mater*., 2003, no. 4, pp. 70–78.
15. Berlin, E.V., Koval, N.N., and Seidman, L.A., *Plazmennaya khimiko-termicheskaya obrabotki poverkhnosti stal'nykh detalei* (Plasma Chemical Thermal Treatment of the Surface of Steel Items), Moscow: Tekhnosfera, 2012.
16. Parancandola, S., Kruse, O., and Muller, W., *J. Appl. Phys. Lett*., 1999, vol. 75, no. 13, p. 1851.
17. Sanchette, F., Damonde, E., Burvron, M., et al., *Surf Coat. Technol*., 1997, vols. 94–95, nos. 1–3, pp. 261–267.
18. Schanin, P.M., Kozyrev, A.V., Koval, N.N., Goncharenko, I.M., Grigoriev, S.V., and Tolkachev, V.S., *J. Tech. Phys*., 2000, vol. 41, no. 2, special issue, pp. 177–184.
19. Schanin, P.M., Kozyrev, A.V., Koval, N.N., Goncharenko, I.M., Langner, J., and Grigoriev, S.V., *Proc. 1st Int. Congress on Radiation Physics, High Current Electronics and Modification of Materials*, Tomsk, Russia, 2000, vol. 3, pp. 438–441.
20. Ivanov, Yu.F., Koval, N.N., Krysina, O.V., et al., *Surf. Coat. Technol*., 2012, vol. 207, pp. 430–434.
21. Lotkov, A.I., Psakh'e, S.G., Knyazeva, A.G., et al., *Nanoinzheneriya poverkhnosti. Formirovanie neravnovesnykh sostoyanii v poverkhnostnykh sloyakh materialov metodami elektronno-ionno-plazmennykh tekhnologii* (Surface Nanoengineering. Formation of Nonequilibrium States in Surface Layers of Materials by Electron Plasma Technology Methods), Novosibirsk: Sib. Otd. Ross. Akad. Nauk, 2008.
22. Musil, J. and Zeman, P., *Solid State Phenom*., 2007, vol. 127, pp. 31–36.
23. Veprek, S., Veprek-Heijman, M.G.J., Karvankova, P., and Prochazka, J., *Thin Solid Films,* 2005, vol. 476, pp. 1–29.
24. Veprek, S. and Reiprich, S., *Thin Solid Films*, 1995, vol. 268, pp. 64–71.
25. Musil, J. and Vlcek, J., *Thin Solid Films*, 1999, vols. 343–344, pp. 47–50.
26. Veprek, S., Veprek-Heijman M.G.J., and Zhang, R., *J. Phys. Chem. Solids*, 2007, vol. 68, pp. 1161–1168.
27. PalDey, S. and Deevi, S.C., *Mater. Sci. Eng.,* 2003, vol. A361, pp. 1–8.
28. Denisov, V.V., Koval, N.N., Lobach, M.I., Mikov, A.V., Shugurov, V.V., and Yakovlev V.V., *Proc. 9th Int. Conf. on Modification of Materials with Particle Beams and Plasma Flows*, Tomsk, Russia, September 21–26, 2008, pp. 31–34.
29. Lopatin, I.V., Akhmadeev, Yu.Kh., Denisov, V.V., Koval, N.N., Mikov, A.V., Yakovlev, V.V., and Seredinin, A., *Izv. Vyssh. Uchebn. Zaved., Fiz*., 2007, no. 9, annex, pp. 98–101.